A Unified Parameterization of Human Gait Across Ambulation Modes

Kyle R. Embry, *Student Member, IEEE,* Dario J. Villarreal, *Student Member, IEEE,*
and Robert D. Gregg, *Senior Member, IEEE*

Abstract— This paper introduces a novel gait parameterization method that models gait kinematics as a continuous function of gait cycle phase, walking speed, and ground slope. Kinematic data was recorded from seven able-bodied subjects walking on a treadmill at twenty-seven combinations of walking speed and ground slope. Convex optimization was used to determine the parameters of a function of three variables that fits this experimental data. This function may be able to provide desired trajectories to a virtual constraint controller over a continuum of gait phases and ambulation modes. This could allow for a single, non-switching controller to control a prosthetic leg for a variety of tasks, avoiding many of the problems associated with the ubiquitous use of finite state machines in prosthesis control.

I. INTRODUCTION

Biped locomotion is an incredibly complicated hybrid dynamic activity, requiring the synchronization of links while providing propulsion, shock absorption, stance stability, and energy conservation across continuously varying ambulation modes or environments. Due to this complexity, analysis of the continuous human gait cycle is traditionally split into different ambulation modes, herein referred to as tasks, and the gait cycles within tasks are further split into distinct periods called phases [1].

Task and gait cycle discretization is also a common practice in the design of controllers for powered prosthetic legs. Most control algorithms will first define a finite number of tasks (e.g., level ground walking, ramp ascent on a specific slope, ramp descent on a specific slope, walking at specific slow, normal, or fast speeds, etc.) and use a finite state machine (FSM) to switch between these tasks using intent recognition [2]–[4]. Each task is further subdivided into periods analogous to those in conventional gait analysis, resulting in a large number of independent tuning parameters [5]–[7]. There are techniques to mitigate the time needed to tune this number of personalized parameters [8], but the FSM method is fundamentally constrained to a discrete set of tasks and gait cycle periods, not the full continuum of possible human locomotion.

[1]K. Embry is with the Department of Mechanical Engineering, D. Villarreal is with the Department of Bioengineering and [2]R. Gregg is with the Departments of Bioengineering and Mechanical Engineering, University of Texas at Dallas, Richardson, TX 75080, USA [1]kyle.embry@utdallas.edu, [2]rgregg@ieee.org

Virtual constraints are an effective technique for the elimination of finite state machines in the field of bipedal robots. A virtual constraint is any constraint on the state space of a system that is enforced through feedback control alone [9]. Virtual constraints help to synchronize the movement of each link of a robot to a phase variable. A phase variable is a mechanical signal that grows monotonically with time in the absence of perturbation. By using virtual constraints, biped robots can successfully ambulate in the presence of terrain variation and velocity perturbations, all with one, non-switching controller [10].

Gregg *et al.* [11] have experimentally demonstrated that using virtual constraints to unify the stance period of gait allows transfemoral amputees to walk at a variety of cadences with just one controller for stance. Recent work has shown that it is possible to robustly parameterize an entire gait cycle with a single phase variable [12], which has been used in the virtual constraint controller of a powered knee-ankle prosthetic leg to achieve steady-state stable gaits in simulation and experiments [13], [14]. However, this controller is designed for one desired joint trajectory at a time and would require the use of a FSM to switch between tasks. For an ankle prosthesis using a lead screw actuator, [15] demonstrates a mapping from percent gait and stride length to desired lead screw position. As stride length is related to forward speed, this mapping could be said to unify the gait cycle across speeds alone. Leroux *et al.* [16] analyzed human gait kinematics at five inclines and two speeds but did not suggest a continuous parameterization for use in control.

The objective of this research is to unify the gait cycle across a range of tasks, specifically walking speeds and inclines. To do so, we will propose a method for the continuous parameterization of human joint kinematics as a function of a phase variable and a task variable. In the context of this paper, a task variable is defined as a multidimensional numeric description of ambulation mode. We will then show an example that suggests that given a sufficient set of kinematic data over a range of tasks we are able to construct a set of gait basis functions. Linear combinations of these gait basis functions accurately describe the training data and can be used to predict kinematics for untrained tasks. This kinematic function could then be implemented into a virtual constraint controller, allowing for robust ambulation across a continuum of gait phases and tasks.

Section II-A and II-B outline the procedure for acquiring and post-processing the kinematic data. Section II-C describes the process of fitting experimental data with gait parameterization functions. Section II-D outlines a procedure to determine the goodness-of-fit of this function to both

the data it was trained on and data withheld from the training process. Section II-E gives a similar algorithm for evaluating an ideal FSM, which will be used as a measure of comparison. Section III fits a gait parameterization function to our experimental data and compares the effectiveness of this function to predict gait kinematics to that of a FSM. Section IV-A and IV-B discuss some interpretations of this method of gait parameterization and how the process can be built upon with convex optimization. Finally, Section IV-C concludes the paper and outlines future work.

II. METHODS

A. Experimental Protocol

The experimental protocol was approved by the Institutional Review Board at the University of Texas at Dallas. All subjects provided written informed consent and self-reported the ability to walk over uneven ground and avoid obstacles with ease. Our subject pool consisted of 7 able-bodied subjects (4 female) with a mean age of 22 years ($\sigma = 2.7$ years), mean height of 167 cm ($\sigma = 6.7$ cm), and mean weight of 61 kg ($\sigma = 7.7$ kg).

Subjects walked for several trials of one minute intervals on an instrumented Bertec treadmill while a 10-camera Vicon motion capture system recorded their lower body kinematics at 100 Hz. During each trial, the subject walked at a constant speed of either 0.8 m/s, 1.0 m/s, or 1.2 m/s (respectively slow, normal, and fast) and a constant ground slope ranging from -10 degrees to +10 degrees at 2.5 degree increments. These inclines were selected to exceed the range of inclines of [16]. The order of all trials was randomized and breaks were taken as needed to prevent fatigue. Each subject walked at every combination of these three speeds and nine inclines, giving a total of 27 trials. For the purpose of this paper, each trial is defined as a separate task and given a unique identifier, θ_j with $j = 1, 2, ..., 27$.

B. Data Processing

To synchronize between strides, the time axis of each stride's kinematic trajectory is normalized from 0 to 1 (i.e., 0%-100% gait) and interpolated to contain $L = 1001$ data points. The normalized time axis can then be interpreted as a discrete phase variable $0 \leq \phi_i < 1$ where $i = 1, 2, ..., L$, and $\phi_{i+1} - \phi_i = \frac{1}{L-1}$.

Human gait has natural variability, so joint angle data is treated as a random variable. The expected value of a measured joint angle for a specific subject at discrete phase variable value ϕ_i and task variable value θ_j is defined as $\mathbf{x}_{\phi_i, \theta_j} \in \mathbb{R}$. The across subject mean at a particular ϕ_i and θ_j value will be referred to as $\bar{\mathbf{x}}_{\phi_i, \theta_j} \in \mathbb{R}$. The standard error between subject means is referred to as $\mathrm{SE}(\mathbf{x}_{\phi_i, \theta_j}) \in \mathbb{R}$.

C. Gait Parameterization

We will now outline how to parameterize a continuous function $q(\phi, \theta)$, where q is the angular position of a joint as a function of phase variable ϕ and task variable θ. The phase variable ϕ is cyclic and bounded ($0 \leq \phi < 1$), where $\phi = 0$ represents the start of a gait cycle, and $\phi = 1$ denotes

the end of that gait cycle and the start of the next. The task variable θ is a vector where each element is a numeric description of ambulation mode. Dimensions of the vector θ could include walking speed, ground slope, stair grade, etc., but in this paper we only consider the first two categories. Our experiments covered 27 combinations of three speeds and nine inclines, resulting in 27 vector values of θ_j.

We begin by modeling $q(\phi, \theta)$ as a scalar, separable function of ϕ and θ:

$$q(\phi, \theta) = \sum_{k=1}^{N} b_k(\phi) c_k(\theta). \tag{1}$$

The index k runs from $1, 2, ..., N$ and denotes the number of $b_k(\phi) \in \mathbb{R}$ and $c_k(\theta) \in \mathbb{R}$ functions used. The gait basis functions, $b_k(\phi)$, map from ϕ to joint kinematics, and will be determined with convex optimization. The task coefficient functions, $c_k(\theta)$, determine the coefficients of the linear combination of gait basis functions for a given task. We explicitly define these coefficient functions before determining the basis functions to ensure intuitive relationships with task. Every $c_k(\theta)$ must be continuous on θ in order to make $q(\phi, \theta)$ continuous on θ. They also must be linearly independent on the discretized domain of θ_j with $j = 1, 2, ..., M$, the tasks used to fit (1) to experimental data. Selecting a large value of N usually decreases the fitting error in this step, but runs the risk of overfitting the data. The author's experience has shown that $N \approx 7$ works well for both the knee and ankle joint, and that polynomials of order ≤ 3 work well for $c_k(\theta)$.

The next objective is to select functions $b_k(\phi)$ such that (1) will approximately fit the experimental data. To do so, we will optimize across $b_k(\phi_i)$ such that

$$\bar{\mathbf{x}}_{\phi_i, \theta_j} \approx \sum_{k=1}^{N} b_k(\phi_i) c_k(\theta_j) \tag{2}$$

$$\forall \ i = 1, 2, ..., L, \ j = 1, 2, ..., M.$$

To incorporate the natural variability of human gait, we will scale the error in degrees, $\bar{\mathbf{x}}_{\phi_i, \theta_j} - b_k(\phi_i) c_k(\theta_j)$, by dividing it by the standard error, $\mathrm{SE}(\mathbf{x}_{\phi_i, \theta_j})$. This will cause our optimization process to fit $b_k(\phi_i) c_k(\theta_j)$ more closely to $\bar{\mathbf{x}}_{\phi_i, \theta_j}$ for values of ϕ_i and θ_j where the standard error is small. Finding the optimal values of $b_k(\phi_i)$ for this objective is easily solved with a linear optimization program (LP). First define the matrices:

$$\bar{\mathbf{X}} = \begin{bmatrix} \bar{\mathbf{x}}_{\phi_1, \theta_1} & \bar{\mathbf{x}}_{\phi_1, \theta_2} & \cdots & \bar{\mathbf{x}}_{\phi_1, \theta_M} \\ \bar{\mathbf{x}}_{\phi_2, \theta_1} & \bar{\mathbf{x}}_{\phi_2, \theta_2} & \cdots & \bar{\mathbf{x}}_{\phi_2, \theta_M} \\ \vdots & \vdots & \ddots & \vdots \\ \bar{\mathbf{x}}_{\phi_L, \theta_1} & \bar{\mathbf{x}}_{\phi_L, \theta_2} & \cdots & \bar{\mathbf{x}}_{\phi_L, \theta_M} \end{bmatrix} \tag{3}$$

$$B = \begin{bmatrix} b_1(\phi_1) & b_2(\phi_1) & ... & b_N(\phi_1) \\ b_1(\phi_2) & b_2(\phi_2) & ... & b_N(\phi_2) \\ \vdots & \vdots & \ddots & \vdots \\ b_1(\phi_L) & b_2(\phi_L) & ... & b_N(\phi_L) \end{bmatrix}$$

$$C = \begin{bmatrix} c_1(\theta_1) & c_1(\theta_2) & ... & c_1(\theta_M) \\ c_2(\theta_1) & c_2(\theta_2) & ... & c_2(\theta_M) \\ \vdots & \vdots & \ddots & \vdots \\ c_N(\theta_1) & c_N(\theta_2) & ... & c_N(\theta_M) \end{bmatrix}$$

$$\mathbf{S} = \begin{bmatrix} \mathrm{SE}(\mathbf{x}_{\phi_1, \theta_1}) & \mathrm{SE}(\mathbf{x}_{\phi_1, \theta_2}) & ... & \mathrm{SE}(\mathbf{x}_{\phi_1, \theta_M}) \\ \mathrm{SE}(\mathbf{x}_{\phi_2, \theta_1}) & \mathrm{SE}(\mathbf{x}_{\phi_2, \theta_2}) & ... & \mathrm{SE}(\mathbf{x}_{\phi_2, \theta_M}) \\ \vdots & \vdots & \ddots & \vdots \\ \mathrm{SE}(\mathbf{x}_{\phi_L, \theta_1}) & \mathrm{SE}(\mathbf{x}_{\phi_L, \theta_2}) & ... & \mathrm{SE}(\mathbf{x}_{\phi_L, \theta_M}) \end{bmatrix}$$

which will be used in the LP. Note that the matrix C needs to be full rank, which creates the previously mentioned constraint that the functions $c_k(\theta)$ must be linearly independent functions on the domain of θ_j with $j = 1, 2, ..., M$. To find an optimal solution for (2), solve the LP:

$$\text{minimize} \quad \rho \quad (4)$$
$$\text{subject to} \quad -\rho \mathbf{S} \preccurlyeq \bar{\mathbf{X}} - BC \preccurlyeq \rho \mathbf{S}.$$

The solution of (4) gives optimal $\rho = \rho^*$ and $B = B^*$. To calculate discrete values of the joint angular position, as in (2), we define $b_k^*(\phi_i)$ as the element in the kth column and i^{th} row of B^* and define the discrete form of (1):

$$q(\phi_i, \theta_j) = \sum_{k=1}^{N} b_k^*(\phi_i) c_k(\theta_j) \in \mathbb{R}. \quad (5)$$

The final step in defining (1) is to fit a continuous function through each vector of discrete values $b_k^*(\phi_i)$ for $i = 1, 2, ..., L$ to form the continuous functions $b_k(\phi)$. As each $b_k(\phi)$ is periodic and real valued, Fourier Interpolation as in [13] should fit the data closely with few coefficients.

D. Evaluating the Parameterization

To evaluate how well (5) can predict untrained tasks, we define the training tasks (or training data) as θ_j with $j = 1, 2, ..., M$, and the validation tasks (or validation data) as θ_j with $j = M + 1, M + 2, ..., P$. For this paper, ten tasks were selected for training ($M = 10$) and seventeen for validation ($P = 27$). The tasks were selected such that one validation tasks lies between each training task, as can be seen in Table I. The validation tasks will be used exclusively to measure how closely (5) can predict untrained tasks and were not used in the fitting process (4). The error between the predicted kinematic value, $q(\phi_i, \theta_j)$, and the real value found via experiments, $\bar{\mathbf{x}}_{\phi_i, \theta_j}$, for task θ_j is defined as:

$$g_j = \max_i \left\{ \frac{\bar{\mathbf{x}}_{\phi_i, \theta_j} - q(\phi_i, \theta_j)}{\text{SE}(\mathbf{x}_{\phi_i, \theta_j})} \right\} \quad (6)$$
$$\forall \ i = 1, 2, ..., L \text{ and } j = 1, 2, ..., P$$

where $q(\phi_i, \theta_j)$ is calculated as in (5). Taking the maximum over i gives the value of the largest error encountered in a gait cycle. This evaluation is repeated for all θ_j, giving an error value g_j for each task. For $j = 1, 2, ...M$, g_j is a measure of how well the training data is fit by (5), and will not exceed ρ^* by definition. For $j = M + 1, M + 2, ..., P$, g_j is a measure of how well we can predict untrained tasks.

TABLE I
TASKS SELECTED FOR TRAINING (DENOTED BY 'X')

Incline (deg)		-10	-7.5	-5	-2.5	0	2.5	5	7.5	10
	0.8	X		X		X		X		X
Speed (m/s)	1									
	1.2	X		X		X		X		X

E. Comparison to Ideal Finite State Machine

The benefit of the proposed parameterization is demonstrated by comparing each g_j from (6) to the performance of a comparable ideal FSM for untrained tasks. We will define such a FSM as one that has been defined with states corresponding to the same set of training data as the gait parameterization method. When provided with an input task, θ_j, the ideal FSM returns a kinematic trajectory of training data ($\mathbf{x}_{\phi_i, \theta_j'}$ with $i = 1, 2, ..., L$) that would most closely match the untrained trajectory for θ_j. The amount of error this method would yield for untrained task θ_j with $j = M + 1, ..., P$ is:

$$g_j = \min_{j'} \left\{ \max_i \left\{ \frac{\bar{\mathbf{x}}_{\phi_i, \theta_j} - \bar{\mathbf{x}}_{\phi_i, \theta_{j'}}}{\text{SE}(\mathbf{x}_{\phi_i, \theta_j})} \right\} \right\} \quad (7)$$
$$\forall \ i = 1, 2, ..., L, \quad j = M + 1, ..., P, \quad j' = 1, 2, ..., M$$

where g_j is the error, which will be compared directly to the values of g_j of the parameterization method. Taking the maximum over i gives the largest error encountered over a gait cycle, while taking the minimum over j' returns the training data trajectory that best fits the untrained task θ_j. Although it may not be possible to achieve this FSM in real time, it is a useful standard of comparison, as it represents the minimum possible error with the FSM approach.

III. RESULTS

A. Parameterizing Experimental Data

In this section, we will parameterize hip, knee, and ankle kinematics and evaluate the ability of the proposed parameterization to predict untrained task kinematics. Percent gait acts as the phase variable of (1), and θ was selected to reflect the two parameters tested in our experiments:

$$\phi = \frac{t}{T}, \quad \phi_i = \frac{t_i}{T}, \quad \theta = [v, \alpha], \quad \theta_j = [v_j, \alpha_j] \quad (8)$$

where t and t_i are continuous and discrete time, respectively, from the beginning of a gait cycle, and T is the total time of a gait cycle. The term v is walking speed in m/s, while α is the ground slope in degrees. Their discrete counterparts, v_j and α_j, are the speed and ground slope of discrete task θ_j.

For each joint parameterization, polynomial functions of θ are chosen for $c_k(\theta)$ for simplicity and continuity. The authors' experience has shown that changes in gait due to difference in ground slope are more complex than changes due to difference in speed, so $c_k(\theta)$ contains higher order polynomials of α than v in the following definitions:

$$c_1(\theta) = v, \quad c_2(\theta) = \alpha, \quad c_3(\theta) = v\alpha, \quad (9)$$
$$c_4(\theta) = v^2, \quad c_5(\theta) = \alpha^2, \quad c_6(\theta) = v\alpha^2, \quad c_7(\theta) = \alpha^3.$$

These are all scalar valued, continuous on θ, and linearly independent functions on the training tasks θ_j with $j = 1, 2, ..., 10$, satisfying all conditions for $c_k(\theta)$. Note that while the same functions $c_k(\theta)$ are used for the hip, knee, and ankle joint in this example, this is not required. The choice of $N = 7$ provides a good compromise of fitting experimental data accurately without overfitting, and during previous testing it was found that a matrix of rank 7 could satisfactorily approximate the experimental data for all tasks. To ensure a simple mapping from gait speed and ground slope to desired trajectories, polynomial functions with rank ≤ 3 were selected for all $c_k(\theta)$. This simplicity is an important design criterion, as in practice the gait coefficient functions will need to be reevaluated for every change in task. Each $c_k(\theta)$ contains only one term, so it is not necessary to

scale these functions with a constant. Solving (4) determines the scale of the corresponding gait basis function for each task coefficient function.

Equation (4) is solved to determine B^* and ρ^*, yielding:

$$\rho^*_{hip} = 0.258 \quad \rho^*_{knee} = 0.325 \quad \rho^*_{ankle} = 0.242. \quad (10)$$

This means that given $b^*_k(\phi_i)$ from B^*, (5) is always within 0.258, 0.325, or 0.242 standard errors of the training data $\bar{\mathbf{X}}$ for the hip, knee, and ankle kinematics, respectively. See the trained tasks in Table II.

B. Evaluating the Parameterization of Experimental Data

Next, we compare the error in our prediction of all tasks, trained and untrained, to the errors that would result from the use of an ideal FSM. Table II shows the mean, max, and standard deviation of the error value g_j for both the parameterization method (6) and the FSM (7). The FSM has zero error on trained tasks ($j=1,2,...,10$) by definition, unlike the parameterization method, which has some minor amount of error after the fitting process because it is a low-rank representation of the training data (see Section IV-A). The power of the parameterization method arises in its ability to predict untrained data ($j=11,12,...,27$). Table II shows that the function $q(\phi_i, \theta_j)$ has about half of the mean and maximum error of the FSM method for the knee and ankle for untrained tasks and around 60% less error for the hip. A one-tailed t-test affirms that the parameterization method has statistically lower error on untrained data for the hip, knee, and ankle with p-levels of 3.54e-4, 0.0052 and 3.68e-6, respectively. See Fig. 1 and Fig. 2 for a comparison between the parameterization's predictions of kinematics at 1.0 m/s (plotted as a continuous surface across phase and ground slope) and untrained kinematic data at 1.0 m/s (plotted as red trajectories over phase at constant ground slopes). The gait parameterization function is simultaneously predicting accurate gait kinematics for an untrained speed, and four untrained ground slopes (-7.5 deg, -2.5 deg, 2.5 deg, and 7.5 deg) in these figures, see Table I.

TABLE II
COMPARISON OF TECHNIQUES

		Trained			Untrained		
		$\bar{g}$	max(g)	$\sigma(g)$	$\bar{g}$	max(g)	$\sigma(g)$
Hip	$q(\phi_i, \theta_j)$	0.237	0.258	0.054	0.333	0.696	0.182
	FSM	0	0	0	0.568	0.906	0.184
Knee	$q(\phi_i, \theta_j)$	0.306	0.325	0.045	0.485	1.286	0.338
	FSM	0	0	0	1.077	3.961	0.830
Ankle	$q(\phi_i, \theta_j)$	0.223	0.242	0.040	0.358	0.676	0.132
	FSM	0	0	0	0.765	1.335	0.285

IV. DISCUSSION AND CONCLUSION

A. Significance

Virtual constraints are a powerful technique for creating robust position based prosthesis controllers, but they require that desired trajectories are known for all tasks the prosthesis will perform. The parameterization technique detailed in this paper could allow a virtual constraint controller to calculate a desired kinematic trajectory on a continuum of tasks. For example, (1) could act as the tracking reference in a PD or feedback linearization control framework as in [9, (6.3)]. A portion of this task continuum can be viewed in Fig. 1 and Fig. 2. The results of Table II indicate that only a small subset of tasks need to be used for training the parameterization, and tasks in between can be interpolated with higher accuracy than using fixed states in a FSM.
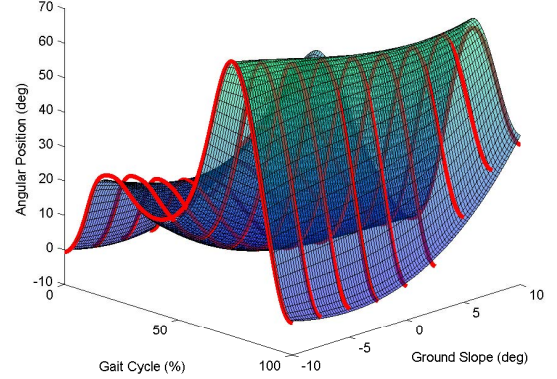

Fig. 1. A surface plot of (5) that has been fit to knee kinematics. In both figures, the speed dimension has been suppressed to a constant, 1.0 m/s and the trajectories shown in red are untrained.
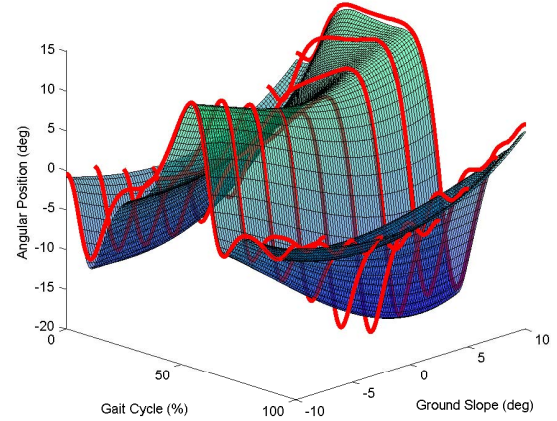

Fig. 2. A surface plot of (5) that has been fit to ankle kinematics.

The continuous gait parameterization method also facilitates an intuitive approach for analyzing how gait kinematics change in response to task changes. The contribution of $b_k(\phi)$ to the kinematic output $q(\phi, \theta)$ is proportional to $c_k(\theta)$. Observations of the functions $b_k(\phi)$ can highlight trends in gait kinematics. Take for example the plot of $b_1(\phi)$ for the ankle in Fig. 3. This gait basis function scales with task coefficient function $c_1(\theta) = v$, and shows that as speed increases, ankle kinematics exhibit additional dorsiflexion and plantar flexion directly before and after toe-off, respectively (around 60% gait [17]). Gait basis function $b_2(\phi)$, shown in Fig. 3, scales with $c_2(\theta) = \alpha$ and adds additional dorsiflexion at heel strike and additional plantar flexion during toe-off in proportion to ground slope. Confirmation of this trend for a discrete set of tasks is shown in [16, Fig. 2]. The relative complexity of $b_k(\phi)$ in comparison to $c_k(\theta)$ helps to motivate the decision that $c_k(\theta)$ is specified by the researcher and
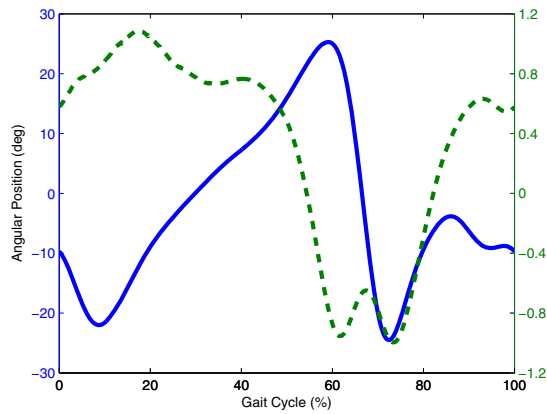
Fig. 3. For the ankle joint, $b_1(\phi)$ is shown as a solid line with scale on the left, and $b_2(\phi)$ is shown as a dashed line with the scale on the right. Note that the magnitude of $b_2(\phi)$ is much smaller than $b_1(\phi)$, but it is multiplied by $c_2(\theta)$, which generally had a larger magnitude than $c_1(\theta)$.

$b_k(\phi)$ is solved for, instead of vice versa.

Another interesting interpretation comes from the selection of the functions $c_k(\theta)$. In (4) it can be seen that if $N < L, M$ (as it was in this paper), then BC is a low rank approximation of the matrix $\bar{\mathbf{X}}$. When the functions $c_k(\theta)$ are selected to be linearly independent on θ_j with $j = 1, 2, ..., M$, these functions form a set of basis vectors, the rows of C, for the data-set. The optimal solution of (4), B^*, gives the coordinates of the data in the basis C that best fit the higher rank matrix $\bar{\mathbf{X}}$. This rank reduction captures a majority of the information in the data-set while simplifying it.

B. Additional Constraints

Adding additional convex constraints to (4) can enforce many properties on the final formula (1) which may be desirable in certain applications. Separate bounds can be placed on each element of the term $\bar{\mathbf{X}} - BC$, which may be useful if some locations are particularly sensitive to error. Due to the use of polynomial expressions for $c_k(\phi)$, it is possible to bound the gradient and higher derivatives of (1) [18]. Moreover, a convex optimization technique called basis pursuit could replace the need for the researcher to explicitly select the functions $c_k(\theta)$. From a predefined dictionary of functions (sometimes called an *over-complete basis*), basis pursuit utilizes ℓ_1-norm regularization to pick a sparse representation.

C. Conclusion

This work introduced a novel gait parameterization method that models gait kinematics as a continuous function of phase and task variable. This parameterization was accurately fit to experimental data with convex optimization. Moreover, it has shown promising results in its ability to accurately predict kinematics for untrained tasks. This flexible framework could enforce additional constraints such as lower error in important regions or a bounded derivative.

The next step for this research is to embed the function (1) as the desired joint angular trajectory in a virtual constraint controller. A prosthesis with this controller could continuously update its kinematic trajectory based upon

measurements of its phase and task. Real-time algorithms may be needed to estimate the variables ϕ and θ, but the parameterization method can easily be retrained for new input variables that correspond to sensor measurements. Our hope is that this parameterization method will allow researchers to create task-invariant virtual constraint controllers for a variety of powered prosthetic devices.

REFERENCES

[1] J. Perry, J. Burnfield, and L. Cabico, *Gait Analysis: Normal and Pathological Function*, 2nd ed. Thorofare, NJ: Slack, 2010.

[2] A. J. Young, A. M. Simon, N. P. Fey, and L. J. Hargrove, "Intent recognition in a powered lower limb prosthesis using time history information," *Ann. Biomed. Engineering*, vol. 42, no. 3, pp. 631–641, 2014.

[3] R. Jiménez-Fabián and O. Verlinden, "Review of control algorithms for robotic ankle systems in lower-limb orthoses, prostheses, and exoskeletons," *Med. Eng. Phys.*, vol. 34, no. 4, pp. 397–408, 2012.

[4] M. R. Tucker, J. Olivier, A. Pagel, H. Bleuler, M. Bouri, O. Lambercy, J. del R Millán, R. Riener, H. Vallery, and R. Gassert, "Control strategies for active lower extremity prosthetics and orthotics: a review," *J. Neuroeng. Rehabil.*, vol. 12, no. 1, p. 1, 2015.

[5] A. M. Simon, K. A. Ingraham, N. P. Fey, S. B. Finucane, R. D. Lipschutz, A. J. Young, and L. J. Hargrove, "Configuring a powered knee and ankle prosthesis for transfemoral amputees within five specific ambulation modes," *PloS one*, vol. 9, no. 6, p. e99387, 2014.

[6] M. F. Eilenberg, H. Geyer, and H. Herr, "Control of a powered ankle–foot prosthesis based on a neuromuscular model," *IEEE T. Neural. Sys. Reh.*, vol. 18, no. 2, pp. 164–173, 2010.

[7] A. H. Shultz, B. E. Lawson, and M. Goldfarb, "Running with a powered knee and ankle prosthesis," *IEEE T. Neur. Sys. Reh.*, vol. 23, no. 3, pp. 403–412, 2015.

[8] A. M. Simon, N. P. Fey, S. B. Finucane, R. D. Lipschutz, and L. J. Hargrove, "Strategies to reduce the configuration time for a powered knee and ankle prosthesis across multiple ambulation modes," in *IEEE Int. Conf. Rehab. Robotics*, Seattle, WA, 2013.

[9] E. R. Westervelt, J. W. Grizzle, C. Chevallereau, J. H. Choi, and B. Morris, *Feedback Control of Dynamic Bipedal Robot Locomotion*. New York, NY: CRC Press, 2007.

[10] B. Griffin and J. Grizzle, "Nonholonomic virtual constraints for dynamic walking," in *IEEE Decis. Contr. P.*, 2015.

[11] R. D. Gregg, T. Lenzi, L. J. Hargrove, and J. W. Sensinger, "Virtual constraint control of a powered prosthetic leg: From simulation to experiments with transfemoral amputees," *IEEE T. Robot.*, vol. 30, no. 6, pp. 1455–1471, 2014.

[12] D. J. Villarreal, H. Poonawala, and R. D. Gregg, "A robust parameterization of human gait paterns across phase-shifting perturbations," *IEEE T. Neur. Sys. Reh.*, 2016, in press.

[13] D. Quintero, A. E. Martin, and R. D. Gregg, "Unifying the gait cycle in the control of a powered prosthetic leg," in *IEEE Int Conf Rehabil Robot.* IEEE, 2015, pp. 289–294.

[14] D. Quintero, D. J. Villarreal, and R. D. Gregg, "Preliminary experiments with a unified controller for a powered knee-ankle prosthetic leg across walking speeds," *IEEE Int. Conf. Intelligent Robot Systems*, 2016, submission.

[15] M. A. Holgate, T. G. Sugar, and A. W. Böhler, "A novel control algorithm for wearable robotics using phase plane invariants," in *IEEE Int. Conf. Robot.* IEEE, 2009, pp. 3845–3850.

[16] A. Leroux, J. Fung, and H. Barbeau, "Postural adaptation to walking on inclined surfaces: I. normal strategies," *Gait & posture*, vol. 15, no. 1, pp. 64–74, 2002.

[17] D. A. Winter, *Biomechanics and motor control of human gait: normal, elderly and pathological*, 1991.

[18] S. P. Boyd and L. Vandenberghe, *Convex Optimization*. New York, NY: Cambridge University Press, 2004.